

Nonperturbative equation of state of quark-gluon plasma. Applications

E.V.Komarov Yu.A.Simonov

*State Research Center Institute of Theoretical and Experimental Physics, Moscow,
117218 Russia*

Abstract

The vacuum-driven nonperturbative factors L_i for quark and gluon Green's functions are shown to define the nonperturbative dynamics of QGP in the leading approximation. EoS obtained recently in the framework of this approach is compared in detail with known lattice data for $\mu = 0$ including P/T^4 , ε/T^4 , $\frac{\varepsilon-3P}{T^4}$. The basic role in the dynamics at $T \lesssim 3T_c$ is played by the factors L_i which are approximately equal to the modulus of Polyakov line for quark L_{fund} and gluon L_{adj} . The properties of L_i are derived from field correlators and compared to lattice data, in particular the Casimir scaling property $L_{adj} = (L_{fund})^{\frac{C_2(adj)}{C_2(fund)}}$ follows in the Gaussian approximation valid for small vacuum correlation lengths. Resulting curves for P/T^4 , ε/T^4 , $\frac{\varepsilon-3P}{T^4}$ are in a reasonable agreement with lattice data, the remaining difference points out to an effective attraction among QGP constituents.

Key words: nonperturbative thermodynamics, quark-gluon plasma

PACS: 12.38.Mh

1 Introduction

Dynamics of Quark Gluon Plasma (QGP) is now of great interest, since numerous results of heavy ion experiments call for strong and possibly nonperturbative forces between quarks and gluons, which cannot be explained in the framework of perturbation theory, see [1] for reviews of recent results and their interpretation.

Email addresses: bartnovsky@itep.ru (E.V.Komarov), simonov@itep.ru (Yu.A.Simonov).

Recently one of the authors has proposed a new approach to the study of the QGP dynamics [2], where the main emphasis was done on the vacuum fields, and the resulting modification of quark and gluon propagators was considered as the first and the basic step in the nonperturbative (NP) treatment of QGP, called Single Line Approximation (SLA).

As a result one obtains NP Equation of State (EoS) of QGP in the form of free quark and gluon terms multiplied by vacuum induced factors. The latter are expressed via the only (nonconfining) colorelectric correlator $D_1^E(x)$ [3] and happened to be approximately equal to the absolute values of Polyakov loops L_{fund}, L_{adj} for quarks and gluons respectively.

Thus all vacuum NP dynamics in this approximation is encoded in L_{fund} , and $L_{adj} = (L_{fund})^{9/4}$ by Casimir scaling [4].

Moreover, the phase diagram was calculated in SLA [5] assuming that the phase transition is again vacuum dominated, *i.e.* a transition from confining vacuum with vacuum energy density $\varepsilon_{conf} \cong -\frac{\beta_0}{32}G_2(conf)$ to the nonconfining vacuum with $\varepsilon_{dec} \cong -\frac{\beta_0}{32}G_2(dec)$.

The resulting phase curve $T_c(\mu)$ in [5] depends on $\Delta G_2 = G_2(conf) - G_2(dec)$ and is in good agreement with lattice data for standard values of $G_2(conf)$ [6] and $\Delta G_2 \approx 0.35 G_2(conf)$.

Thus the SLA is a reasonable starting point with no fitting or model parameters, since L_{fund} can be computed analytically [3,7] or on the lattice [8,9], and ΔG_2 is the fundamental parameter of QCD [5]. This picture of the QCD phase transition was called in [5] the Vacuum Dominance Model (VDM) originally proposed in [10] in a simplified form (sometimes called the Evaporation Model).

In the model the basic element of the NP dynamics of QGP is the quark and gluon Polyakov lines, which are connected to each other by Casimir scaling. It is the purpose of this paper to study in detail properties of Polyakov lines with the help of the Field Correlator Method (FCM) [11] where those can be derived from the nonvanishing colorelectric field correlator D_1^E . In particular, $D_1^E(x)$ can be derived from the gluelump Green's function, and the latter was calculated analytically in [7,12] and on the lattice the gluelump spectrum was found in [13]. These properties can be compared to the lattice data both at $T \leq T_c$ and $T > T_c$, and we predict behaviour of L_{fund}, L_{adj} at $T \leq T_c$ which violates Casimir scaling for $n_f = 0$, since there $L_{fund} \equiv 0$ and $L_{adj} = \exp\left(-\frac{m}{T}\right)$, with m – known gluelump mass. At $T \geq T_c$ Casimir scaling follows from the dominance of quadratic (Gaussian) correlator, and we estimate the admixture of higher correlators, violating the scaling.

At this point we notice, that contribution of bound states of static quark or static adjoint charge with gluons in QGP to the lattice defined $F_s(\infty, T)$ and consequently to L_{fund}, L_{adj} would violate Casimir scaling, and the accurate observation of Casimir scaling in [4] thus poses some limits on those bound states.

As a result we fix the form of L_{fund}, L_{adj} based on our analytic and lattice calculations and enter with those to compute EoS, *i.e.* $P(T), \varepsilon(T)$ and their derivatives. Results of these computations are compared with numerous lattice data and shown to agree reasonably well within the accuracy of lattice simulations.

The paper is organized as follows. In section 2 basic thermodynamic equations for QGP are derived, and natural appearance of Polyakov loops in EoS is derived. In doing so an economic expression for the gluon pressure is first obtained, while that of quarks is taken from [2].

In section 3 the expressions for L_{fund}, L_{adj} are derived in terms of field correlator D_1^E and finally in terms of the gluelump Green's function and properties of L_{fund}, L_{adj} both below and above T_c are discussed in detail in comparison with lattice data.

In section 4 EoS, $P(T)$ for $n_f = 2, 2 + 1, 3$, $\varepsilon(T)$ and nonideality $\frac{\varepsilon - 3P}{T^4}$ are calculated using the formulas of section 2 and compared to the lattice data.

Section 5 is devoted to the discussion of results and conclusions.

2 Derivation of EoS for quark-gluon plasma

Our derivation below is based on the formalism suggested in [2], where the Background Perturbation Theory (BPTh) is exploited, originally worked out in [14] and developed in connection to the FCM in [15] for $T = 0$ and in [16] for $T > 0$. Correspondingly one splits the gluonic field A_μ into background part B_μ and valence gluon part a_μ , as

$$A_\mu = B_\mu + a_\mu \tag{1}$$

and writes the partition function $Z(B, T)$ as

$$Z(B, T) = N \int D\phi \exp\left(-\int_0^\beta dt \int d^3x L_{tot}(x, t)\right) \tag{2}$$

where ϕ denotes all set of fields a_μ, ψ, ψ^+ and ghost fields. In the lowest order in ga_μ one obtains the result in the so-called Single Line Approximation

$$Z(B, T) = N_1 [\det(G^{-1})]^{-1/2} \det(-D_\lambda^2(B)) [\det(m_q^2 - \hat{D}^2(B - \frac{i\mu_q}{g}\delta_{\mu 4}))]^{1/2} \quad (3)$$

where N_1 is normalization constant, $D_\lambda(B) = \partial_\lambda - igB_\lambda$, $G^{-1} = D_\lambda^2\delta_{\mu\nu} + 2igF_{\mu\nu}$. In what follows we put $\mu_q = 0$, and consider the case $\mu_q \neq 0$ in a subsequent paper [17].

The thermodynamic potential $F(T)$ is connected to $Z(B, T)$ in a standard way

$$F(T) = -T \ln \langle Z(B, T) \rangle_B \quad (4)$$

where the subscript B in $\langle Z \rangle_B$ implies averaging over all background fields. As a result $F(T)$ in SLA is a sum of gluon and quark degrees of freedom separately, $F(T)_{SLA} = F_q(T) + F_{gl}(T)$. In what follows we omit the subscript SLA, since all results (except for corrections to Polyakov lines in the next section) will be valid in this approximation. Using the Fock-Feynman-Schwinger (FFS) path integral formalism (see [18] for reviews) one has a convenient representation

$$\begin{aligned} \frac{1}{T} F_{gl}(T) = Sp \left\{ -\frac{1}{2} \int_0^\infty \frac{ds}{s} \xi(s) e^{-sG^{-1}} + \int_0^\infty \frac{ds}{s} \xi(s) e^{-sD^2(B)} \right\} = \\ - \int_0^\infty \frac{ds}{s} \xi(s) d^4x (Dz)_{xx}^w e^{-K} \left(\frac{1}{2} tr \langle \hat{\Phi}_F(x, x) \rangle_B - \langle tr \hat{\Phi}(x, x) \rangle_B \right) \end{aligned} \quad (5)$$

Here

$$\hat{\Phi}_F(x, y) = P_F P \exp \left(ig \int_y^x B_\mu dz^\mu \right) \exp \left(2ig \int_0^s F(z(\tau)) d\tau \right) \quad (6)$$

and $\hat{\Phi}(x, y)$ is the same as in (6) without the last factor. $\xi(s)$ in the regularizing factor, for details see [2,16]. A similar representation for quarks and antiquarks looks like [16]

$$\frac{1}{T} F_q(T) = -\frac{1}{2} tr \int_0^\infty \frac{ds}{s} d^4x \xi(s) (\overline{Dz})_{xx}^w e^{-K-sm^2} W_\sigma(C_n) \quad (7)$$

Note that in (5),(7) is present the "winding path measure", introduced in [16], e.g. for quarks

$$\begin{aligned} (\overline{Dz})_{xx}^w = \\ \lim_{N \rightarrow \infty} \prod_{n=1}^\infty \sum_{n=0}^\infty (-1)^n \frac{d^4p}{(2\pi)^4} \exp \left\{ ip_\mu \left(\sum_{m=1}^\infty \zeta_\mu(m) - (x-y)_\mu - n\beta\delta_{\mu 4} \right) \right\} \end{aligned} \quad (8)$$

And the same for gluons, $(\overline{Dz})_{xy}^w$ but without the $(-1)^n$ factor. At this point we are posing to contemplate the structure of our result (5),(7) and recognize

that it is a sum of individual quark or individual gluon lines (Green's functions in background) over paths from $(\vec{x}, 0)$ to $(\vec{x}, n\beta)$.

It is clear that for $T < T_c$ this contribution should vanish because of confinement, and one should look into the representation containing gauge invariant Green's functions. These come from white systems, e.g. for singlet (gg) or $(q\bar{q})$ and the corresponding partition function has the form

$$Z^{(n)}(\vec{x}_1, \vec{x}_2) = \int d\Gamma_1 d\Gamma_2 \langle \text{tr} W(C_n^{(1)}, C_n^{(2)}) \rangle \quad (9)$$

where $d\Gamma_i$ are phase space factors. Note the coinciding indices in $W(C_n^{(1)}, C_n^{(2)})$, which denotes the closed Wilson loop (with possible insertions of $F_{\mu\nu}$ and $\sigma_{\rho\lambda} F_{\rho\lambda}$ for quarks) starting at points $(\vec{x}_1, 0)$, $(\vec{x}_2, 0)$ (connected by a parallel transporter) and ending at points $(\vec{x}_1, n\beta)$, $(\vec{x}_2, n\beta)$ (again connected). Now, as was shown in [2], in the deconfined phase the pair partition function factorizes in the leading approximation of $(ga_\mu)^n$, while the color-electric correlator D_1^E yields nonzero contribution to each quark or gluon in the form of Polyakov lines. The derivation is shortly as follows (see [2] for details).

The Wilson loop in (9) can be calculated in terms of field correlators using cluster expansion theorem [19]

$$\begin{aligned} \frac{1}{N_c} \text{tr} \langle W(C_n^{(1)}, C_n^{(2)}) \rangle &= \frac{1}{N_c} \text{tr} \langle P \exp \left(ig \int_{C_n} B_\mu dz^\mu \right) \rangle_B = \\ \exp \left(- \sum_{k=2}^{\infty} \frac{(ig)^k}{k!} \int \int_{S_n} ds_{\mu_1 \nu_1}(u_1) \dots ds_{\mu_k \nu_k}(u_k) D_{\mu_1 \nu_1 \dots \mu_k \nu_k}(u_1, \dots, u_k) \right) \end{aligned} \quad (10)$$

where C_n is the total closed loop, containing $C_n^{(1)}, C_n^{(2)}$ and parallel transporters from \vec{x}_1 to \vec{x}_2 and back, S_n is a surface inside C_n , while the field correlators are defined as follows, e.g. for $k = 2$ (Gaussian approximation) one has

$$D_{\mu_1 \nu_1 \mu_2 \nu_2}(u_1, u_2) = \frac{g^2}{N_c} \text{tr} \langle F_{\mu_1 \nu_1} \Phi(u_1, u_2) F_{\mu_2 \nu_2} \Phi(u_2, u_1) \rangle \quad (11)$$

In what follows we concentrate on color-electric correlators, which can be written in terms of two scalar functions $D^E(w), D_1^E(w)$ (for contribution of other color-magnetic correlators see [2,20]). Note that latter do not produce factorized contribution, but can support weakly bound states with angular momentum $L > 0$)

$$\begin{aligned} D_{i4,k4}(x, y) &= \frac{g^2}{N_c} \langle \text{tr} E_i(x) \Phi(x, y) E_k(y) \Phi(y, x) \rangle = \\ &\delta_{ik} (D^E + D_1^E + u_4^2 \frac{\partial D_1^E}{\partial u_4^2}) + u_i u_k \frac{\partial D_1^E}{\partial u^2} \end{aligned} \quad (12)$$

where $D^E \equiv D^E(u)$, $D_1^E \equiv D_1^E(u)$, $u = x - y$.

We now take into account according to [7,12] that correlation lengths λ^E and λ_1^E , defined from asymptotics $D^E(u) \sim \exp(-|u|/\lambda^E)$, $D_1^E \sim \exp(-|u|/\lambda_1^E)$, are small, $\lambda^E, \lambda_1^E < 0.2$ fm. Indeed from the gluelump correlators [12,13] it follows that $\lambda^E \approx 0.08$ fm, $\lambda_1^E \approx 0.16$ fm. Then for temperatures $T < 1/\lambda^E$, $1/\lambda_1^E$ the n dependence appears explicitly [2] and one can write

$$\frac{1}{N_c} \text{tr} \langle W(C_n^{(1)}, C_n^{(2)}) \rangle = \exp(-w_n^{(2)} - w_n^{(4)} - \dots) \quad (13)$$

where the Gaussian contribution is expressed via D^E , D_1^E

$$w_n^{(2)} = n\beta (V_D(r, T) + V_1(r, T)) \quad (14)$$

and we have defined [2,3]

$$V_D(r, T) = 2 \int_0^\beta d\nu (1 - \nu T) \int_0^r (r - \xi) d\xi D^E(\sqrt{\xi^2 + \nu^2}) \quad (15)$$

$$V_1(r, T) = 2 \int_0^\beta d\nu (1 - \nu T) \int_0^r \xi d\xi D_1^E(\sqrt{\xi^2 + \nu^2}) \quad (16)$$

Here $r = |\vec{x}_1 - \vec{x}_2|$.

Now it is clear, that in the confined regime, when D^E is nonzero, $V_D(r, T)$ grows linearly with r , and factorization of $Z^{(n)}(C_n^{(1)}, C_n^{(2)})$ is impossible - gg and $q\bar{q}$ propagate as hadrons. For $T > T_c$, however, $D^E \equiv 0$ and

$$V_1(r, T) = V_1(\infty, T) + v(r, T) \quad (17)$$

where $v(r, T)|_{r \rightarrow \infty} = 0$ and contains both perturbative and NP contributions. In [9] it was shown that $v(r, T)$ is able to support weakly bound states of heavy quark and antiquark ($Q\bar{Q}$), as well as (gg) and Qg systems. This is in agreement with lattice data [21]. In the SLA approximation we neglect in the first step the effect of $v(r, T)$ and keep only $V_1(\infty, T)$. As will be shown below this latter contribution explains EoS of QGP with good accuracy. Then the gauge invariant quark-antiquark Green's function factorizes into a product of one-body terms, each obtaining a factor

$$L_{fund}^{(n)} \cong \exp\left(-n \frac{V_1(\infty, T)}{2T}\right) = \left(L_{fund}^{(1)}\right)^n \quad (18)$$

For the gluon gg system one obtains in addition in the exponent the Casimir factor $\frac{C_2(adj)}{C_2(fund)} = \frac{9}{4}$, which follows from (10)-(12), when all fields are in the adjoint representation,

$$L_{adj}^{(n)} = \exp\left(-n \frac{9V_1(\infty, T)}{8T}\right) \quad (19)$$

In the next section we study these factors in more detail and establish their relation to the Polyakov loop factors measured on the lattice. We end this section with the discussion of higher correlators in (10).

Keeping for smooth surfaces only even power correlators (see discussion in [22]) one can estimate the contribution of the $k = 4$ correlator compared to the Gaussian one in the exponent of (10) as giving additional factor

$$\eta = \frac{w_n^{(4)}}{w_n^{(2)}} = \overline{(gF)^2} (\lambda^E)^4 \approx \sigma_E (\lambda_E)^2 \sim \frac{0.2 \text{ GeV}^2}{(2 \text{ GeV})^2} < 0.1 \quad (20)$$

where in confinement phase we have estimated $\overline{(gF)^2}$ from the string tension $\sigma_E = \frac{1}{2} \int d^2x D^E(x) \approx \overline{(gF)^2} \overline{(\lambda^E)^2} \approx 0.2 \text{ GeV}^2$. Note that estimate of $\overline{(gF)^2}$ from the gluonic condensate yields η order of magnitude smaller. The estimate (20) gives a reasonable explanation of the good accuracy of Casimir scaling in the confined phase (see [23] for discussion). In the case of deconfinement, when $\sigma_E = 0$ and gluonic condensate is roughly twice as small (up to $T \approx 1.5T_c$ [8]) the "Casimir expansion parameter" η should be even smaller, since λ_1^E does not change significantly [8], while λ_1^H, λ^H stay constant in this region.¹

We obtain doing path integrals as explained in [2],

$$P_{gl} = \frac{N_c^2 - 1}{16\pi^2} \int_0^\infty \frac{ds}{s^3} \sum_{n \neq 0} e^{-\frac{n^2 \beta^2}{4s}} L_{adj}^{(n)} \quad (21)$$

$$P_q = n_f \frac{N_c}{4\pi^2} \int_0^\infty \frac{ds}{s^3} e^{-m_q^2 s} \sum_{n=1}^\infty (-1)^{n+1} e^{-\frac{n^2 \beta^2}{4s}} L_{fund}^{(n)} \quad (22)$$

Finally performing integration over ds one has

$$P_{gl} = \frac{2(N_c^2 - 1)}{\pi^2} T^4 \sum_{n=1}^\infty \frac{1}{n^4} L_{adj}^n \quad (23)$$

$$P_q = \frac{4N_c n_f}{\pi^2} T^4 \sum_{n=1}^\infty \frac{(-1)^{n+1}}{n^4} L_{fund}^n \varphi_q^{(n)} \quad (24)$$

where we have defined $L_{adj} \equiv L_{adj}^{(1)}$, $L_{fund} \equiv L_{fund}^{(1)}$, see (18),(19), and

$$\varphi_q^{(n)} = \frac{n^4}{16T^4} \int_0^\infty \frac{ds}{s^3} e^{-m_q^2 s - \frac{n^2 \beta^2}{4s}} = \frac{n^2 m_q^2}{2T^2} K_2\left(\frac{nm_q}{T}\right) \quad (25)$$

These equations and another, integral form instead of the infinite sum, will be used in section 4 to compare with lattice data.

¹ Note that estimate (20) refers to the plane or at least smooth surface, while for a crumpled surface higher correlators play important role to make area law with the minimal surface.

3 Polyakov lines and field correlators

Below only quadratic (Gaussian) field correlators are considered, basing on the Casimir scaling property which these correlators ensure, and being in agreement with lattice data both for $T = 0$ [23] and for $T > T_c$ [4]. At $T > 0$ four Gaussian correlators are $D^E(x)$, $D_1^E(x)$, $D^H(x)$, $D_1^H(x)$, with $\sigma^{E,H} = \frac{1}{2} \int D^{E,H}(x) d^2x$. At $T > T_c$ the correlator D^E and σ^E vanish, as was suggested in [10] and proved on the lattice [8], and three other correlators are nonzero, moreover the spatial string tension $\sigma_s \equiv \sigma^H$ grows with temperature in the dimensionally reduced limit [24]. This fact explains also the growth with temperature of the Debye mass, $m_D \cong 2\sqrt{\sigma_s}$ [25], which is known from lattice data [24]. Apart from this quantity, we shall not use below the colormagnetic correlators, since they do not produce static potentials for interparticle angular momentum $L = 0$.

Therefore we shall be interested only in color-electric (CE) correlators $D^E(x)$ (inside the confining phase bounded by the curve $T_c(\mu)$), and $D_1^E(x)$ in the whole μ, T plane.

It is important at this point to stress that in our approach only gauge invariant states $|n\rangle$ are to be considered in the partition function at $T > 0$,

$$Z = \sum_n \langle n | e^{-H/T} | n \rangle \quad (26)$$

as well as in all QCD states at $T = 0$. This is evident in the confining phase, since a colored part of the gauge invariant system is connected by the string to other parts.

With the lack of string in the deconfined phase the necessity of using the gauge invariant amplitudes is less evident, except for worldlines in the spatial directions, where colormagnetic confinement with nonzero σ_s is operating.

Nevertheless our use of gauge invariant amplitude, which factorizes at large interparticle distances in the deconfined phase, leads to the explicit prediction of EoS with modulus of phase factors, which approximately equal to modulus of Polyakov lines.

Below we shall use, as in [2,5], the gauge invariant states, $|n\rangle$ at all μ, T and we shall express the interparticle dynamics in terms of gauge invariant quantities, like pair or triple static potentials. The large distance limit of these potentials yields one-particle characteristics – the self-energy parts of quarks, antiquarks, gluons etc. One can use those to study thermodynamics of QGP in the one-particle, or Single Line Approximation (SLA) [2]. It is rewarding, that the field correlator method is a natural instrument in describing this deconfined dynamics, since in absence of D^E the correlator D_1^E has the form of the full

derivative and produces gauge invariant one-particle pieces – self-energy parts – automatically (in addition to interparticle interaction decreasing at large distances).

The gauge invariant states $|n\rangle, \langle n|$ formed with the help of parallel transporters (Schwinger lines) $\Phi(x, y) \equiv P \exp(ig \int_y^x A_\mu dz_\mu)$, create, as shown in [2], Wilson loops $W(C)$ for $q\bar{q}, qq\bar{q}$, or else $(qq\bar{q}\bar{q})$ systems. From the latter, as shown in [2,3], one obtains static potentials. When treating colored systems like (qq) , the latter is taken as a part of gauge invariant system $(qq\bar{q}\bar{q})$, and the pairs (qq) and $\bar{q}\bar{q})$ are separated at large distance where potential $V(qq, \bar{q}\bar{q})$ is neglected.

We start with the color singlet $q\bar{q}$ system and write contributions of D^E, D_1^E at nonzero $T = 1/\beta$ to the static potentials [3]

$$V_1(r, T) = \int_0^\beta d\nu(1 - \nu T) \int_0^r \xi d\xi D_1^E(\sqrt{\xi^2 + \nu^2}) \quad (27)$$

$$V_D(r, T) = 2 \int_0^\beta d\nu(1 - \nu T) \int_0^r (r - \xi) d\xi D^E(\sqrt{\xi^2 + \nu^2}) \quad (28)$$

It is important that V_1, V_D give the contribution to the modulus of Polyakov loops, namely [3]

$$L_{fund}^{(V)} = \exp\left(-\frac{V_1(T) + 2V_D}{2T}\right), \quad L_{adj}^{(V)} = (L_{fund}^{(V)})^{9/4} \quad (29)$$

where $V_1(T) \equiv V_1(\infty, T)$, $V_D \equiv V_D(r^*, T)$ and r^* is an average distance between the heavy quark line and light antiquark (for $n_f > 0$), or “heavy gluon line” and a gluon for L_{adj} . The Casimir scaling relation (29) predicted in [3] is in good agreement with lattice data [4], as well as vanishing of L_{fund} for $T \leq T_c, n_f = 0$ and the strong drop of L_{adj} for $T \leq T_c$. Indeed, for $T \leq T_c$ and $n_f = 0$ one has $r^* \rightarrow \infty$ and $V_D \rightarrow \infty$, explaining the vanishing of $L_{fund}^{(V)}$. For $L_{adj}^{(V)}$ in this region one can take into account the kinetic energy of the gluon in the system adjoint source plus gluon in a gluelump. This yields an estimate $L_{adj}(T \leq T_c) = \exp(-\frac{m_{glp}}{T})$, where m_{glp} was computed in [12,13] to be ≈ 1 GeV.

In [3] it was mentioned, that Polyakov lines measured repeatedly on the lattice, are expressed through the (singlet) free energy of $Q\bar{Q}$ system at large distances $F_{Q\bar{Q}}^1(\infty, T)$ in the same way as in (29), i.e

$$L_{fund}^{(F)} = \exp\left(-\frac{F_{Q\bar{Q}}^1(\infty, T)}{2T}\right) \quad (30)$$

and actually the difference between $L_j^{(F)}$ and $L_j^{(V)}$ was not taken into account in [3]. This difference can be easily seen in the standard representation of

$$F_{Q\bar{Q}}^1(r, T)$$

$$\exp\left(-\frac{F_{Q\bar{Q}}^1(r, T)}{T}\right) = \sum_{n(Q\bar{Q})} c_n \exp\left(-\frac{V_n^{Q\bar{Q}}(r, T)}{T}\right) \quad (31)$$

where $n(Q\bar{Q})$ denote all excited and bound states where $Q\bar{Q}$ participate, and $V_n^{Q\bar{Q}}(r, T)$ is the energy term of such state n when distance between static charges Q and \bar{Q} is equal to r . It is clear that $L_j^{(V)}$ coincides with $L_j^{(F)}$ when all states n except for the ground state $n = 0$ are neglected. In this case $V_0^{Q\bar{Q}}(r, T)$ coincides with $V_1(r, T)$, and hence with $F_{Q\bar{Q}}^1(r, T)$. Note at this point, that $V_1(r, T)$ in (27) does not depend on T in the limit when the vacuum correlation length $\lambda(D_1^E(x) \sim e^{-x/\lambda})$ tends to zero, $T \ll \frac{1}{\lambda} \approx 1$ GeV.

In the general case all states $n(Q\bar{Q})$ contribute and therefore ($c_n > 0$) one has inequality

$$V_1(r, T) \geq F_{Q\bar{Q}}^1(r, T) \quad (32)$$

To define V_1 and L_{fund} properly, one should separate perturbative and NP parts and renormalize V_1 to get rid of perimeter divergences.

The separation in $D_1^E(x)$ can be seen at small x [7]

$$D_1^E(x) = \frac{4C_2(f)\alpha_s}{\pi} \left\{ \frac{1 + O(\alpha_s \ln^k x)}{x^4} + \frac{\pi^2 G_2}{24N_c} + \dots \right\} = D_1^{E \text{ pert}}(x) + D_1^{(np)}(x) \quad (33)$$

and at large x , $D_1^{(np)}(x)$ is [7].

$$D_1^{(np)}(x) \cong A_1 \frac{e^{-M_0|x|}}{\sqrt{x^2}}, A_1 = C(f)\alpha_s 2M_0\sigma_{adj} \quad (34)$$

where M_0 is the lowest gluelump mass [12,13], $M_0 \approx 1$ GeV.

The corresponding separation of $V_1(r, T)$ is done in [3,9] as follows

$$V_1(r, T) = V_1^{pert}(r, T) + V_1^{(np)}(r, T) + V_1^{(div)}(a) \quad (35)$$

where

$$V_1^{(pert)}(r, T) = -\frac{C(f)\alpha_s}{r} e^{-m_D r} (1 + O(rT)) \quad (36)$$

$V^{(np)}$ is as in (27) with $D_1^E \rightarrow D_1^{np}(x)$,

$$V_1^{(div)}(a) \cong \frac{2C(f)\alpha_s}{\pi} \left(\frac{1}{a} + O(T \ln a) \right) \quad (37)$$

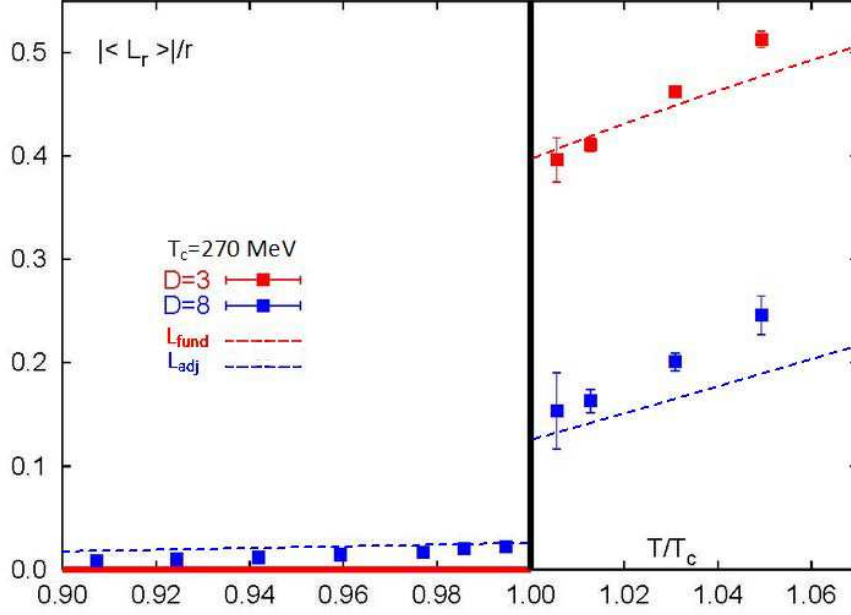


Fig. 1. Shown on the figure are curves of L_{adj} (blue dashed) and L_{fund} (red dashed) compared to the ones taken from [4]. In the $T < T_c$ region the $M(\bar{\alpha}_s = 0.195) = 0.982$ GeV gluelump mass was used. In the deconfinement region the fit (39) was used with $T_c = 270$ MeV for L_{fund} and the Casimir scaled value for L_{adj} .

Here $m_D = m_D(T) \approx 2\sqrt{\sigma_s}$ is the np Debye mass [25], and a is the lattice cut-off.

The renormalization procedure suggested in [3] amounts to discarding $V_1^{(div)}(a)$, and this is in agreement with the lattice renormalization used in [26], where $F_{Q\bar{Q}}^1(r, T)$ was adjusted to the form $V_1^{pert}(r, T)$ at small r and T . Note, that $V_1^{np}(r, T) \sim O(r^2)$ in this region and the procedure indeed allows to eliminate the constant term $V_1^{div}(a)$.

We start with the one-particle limit of $V_1(r, T)$, and the corresponding contribution to $L_{fund}^{(V)}$.

According to the discussion above, one defines the renormalized Polyakov loop as in (29),(35) with $V_1(T) \equiv V_1^{np}(\infty, T)$ and we shall neglect the difference between L_j^V and $L_j^{(F)}$ (important at large T , where $L_{fund}^F > 1$, while always $L_{fund}^V < 1$).

From (34) one has (at $T \leq T_c$)

$$V_1^{(np)}(\infty, T) = \frac{A_1}{M_0^2} \left[1 - \frac{T}{M_0} \left(1 - e^{-\frac{M_0}{T}} \right) \right] \quad (38)$$

so that $V_1^{(np)}(\infty, T_c) \approx \frac{6\alpha_s(M_0)\sigma_f}{M_0} \approx 0.5$ GeV for $M_0 \approx 1$ GeV [12,13].

The same type of estimate one obtains from lattice data [27] where at $T \gtrsim T_c$ one can parametrize the data as follows

$$F_{Q\bar{Q}}^1(\infty, T) \approx \frac{1.75}{1.35 \left(\frac{T}{T_c}\right) - 1}, F_{Q\bar{Q}}^1(\infty, T_c) \approx 0.5 \text{ GeV} \quad (39)$$

Thus one can say that quarks (and antiquarks) have selfenergy parts $\kappa_q(T) = \kappa_{\bar{q}}(T) = \frac{1}{2}V_1(T) \approx \frac{1}{2}F_{Q\bar{Q}}^1(\infty, T) \approx 0.25 \text{ GeV}$ at $T \approx T_c$.

To illustrate our discussion of V_D , V_1 and L_{fund} , L_{adj} we show in Fig.1 our curves for L_{fund} , L_{adj} computed from (29) with $V_1(\infty, T) = F_{Q\bar{Q}}^1(\infty, T)$ taken from (16) for $T > T_c$ while $L_{adj} = \exp(-\frac{M_0}{T})$ for $T \leq T_c$. Our dashed curves are plotted in Fig.1 in comparison to lattice data from [4].

For gluons one has instead $\kappa_g(T) = \frac{9}{4}\kappa_q \approx 0.56 \text{ GeV}$. Let us turn now to the r -dependence of interaction. The perturbative part has a standard screened Coulomb behaviour (36), while the NP part vanishes at small r ;

$$V_1^{np}(r, T) \sim \text{const} \cdot r^2, \quad r \rightarrow 0 \quad (40)$$

From (27),(34) one has as in [3]

$$V_1^{(np)}(r, T) = V_1^{(np)}(\infty, T) - \frac{A_1}{M_0^2} K_1(M_0 r) M_0 r + O\left(\frac{T}{M_0}\right) \equiv V_1^{(np)}(\infty, T) + v(r, T) \quad (41)$$

Hence the NP interaction in the white system $Q\bar{Q}$ changes from $V_1^{np}(\infty, T) \approx 0.5 \text{ GeV}$ at large r to zero at small r . The same (multiplied by $\frac{9}{4}$) is true for the white gg system.

We end up this section by discussion of the role of excited states in definition of $F_{Q\bar{Q}}^1$ and possible violation of Casimir scaling for L_{fund} , L_{adj} . It is clear that in $F_{Q\bar{Q}}^1$ for $n_f = 0$ the only possible excited states consist of gluons $(Qg)(\bar{Q}g)$; $(Qgg)(\bar{Q}gg)$ etc. As it was shown in [9], the weakly bound states (Qg) indeed are supported by $V_1(r, T)$, and neglecting the small binding energy the total energy of these states is roughly the sum of selfenergy parts κ_Q and κ_g

$$E_{Qg} \approx \frac{1}{2}V_1(\infty, T) + \frac{9}{8}V_1(\infty, T) \approx 0.8 \text{ GeV} (T \approx T_c) \quad (42)$$

This should be compared to the possible bound state of an adjoint static source G plus gluon, which in the weakly binding limit can be written as

$$E_{Gg} \approx 2 \cdot \frac{9}{8}V_1(\infty, T) \approx 1.1 \text{ GeV} (T \approx T_c) \quad (43)$$

In addition multiplicities of states (42) and (43) are different, which leads to different predictions for corrections to $F_{Q\bar{Q}}^1$ and F_{GG}^1 , not connected by Casimir scaling, in contrast to the main (ground state) term $V_{Q\bar{Q}}^1 = V_1(\infty, T)$ and $V_{GG}^1 = \frac{9}{4}V_1(\infty, T)$. Therefore one expects violation of Casimir scaling by gluon-induced bound states in L_{fund} and L_{adj} , and high accuracy of lattice data [4] indicates then a small role of such bound states.

4 A comparison to the lattice data

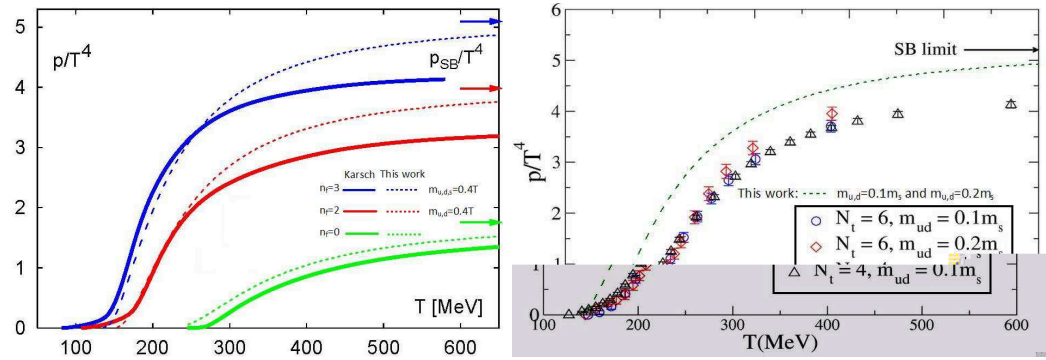


Fig. 2. Pressure $\frac{P}{T^4}$ as function of temperature T . Shown on the left figure is a comparison of the analytical calculus (48),(49) (dashed lines) with the lattice results (bold lines) [28] for the case $n_f = 0, 2, 3$. Shown on the right figure is the case of $n_f = 2 + 1$. Green dashed line is the analytical calculation (48),(49) compared to the lattice one from [29].

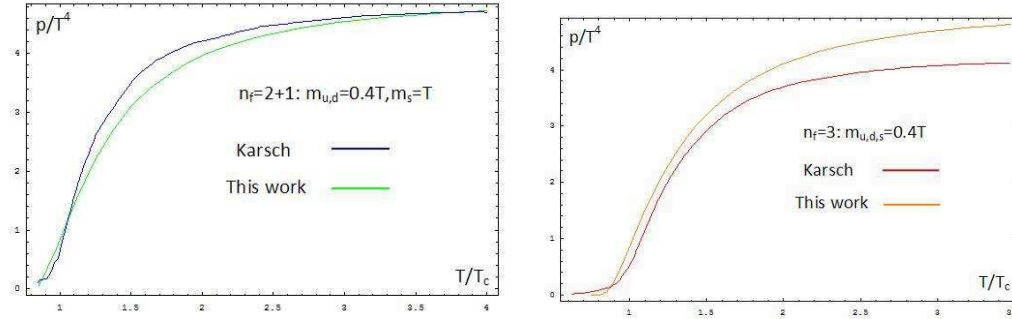


Fig. 3. Pressure $\frac{P}{T^4}$ as function of temperature T . The case of $n_f = 2 + 1$ (left figure) and $n_f = 3$ (right figure) (48),(49). Lattice results were taken from [30].

In this section we shall exploit the reduced pressure $p = \frac{P}{T^4}$, which for $\mu > 0$ can be written as:

$$p_q \equiv \frac{P_q^{SLA}}{T^4} = \frac{4N_c n_f}{\pi^2} \sum_{n=1}^{\infty} \frac{(-1)^{n+1}}{n^4} L_{fund}^n \varphi_q^{(n)} \cosh \frac{\mu n}{T} \quad (44)$$

$$p_{gl} = \frac{P_{gl}^{SLA}}{T^4} = \frac{2(N_c^2 - 1)}{\pi^2} \sum_{n=1}^{\infty} \frac{1}{n^4} L_{adj}^n \quad (45)$$

with $\varphi_q^{(n)}$ given in (25)

$$\varphi_q^{(n)} = \frac{n^2 m_q^2}{2T^2} K_2 \left(\frac{nm_q}{T} \right) \quad (46)$$

Both sums can be written in a more convenient way. Using the representation of K_2 ,

$$\varphi_q^{(n)} = \frac{n^4}{6} \int_0^{\infty} \frac{z^4}{\sqrt{z^2 + \nu^2}} e^{-n\sqrt{z^2 + \nu^2}} dz \quad (47)$$

where $\nu = m_q/T$, one has²:

$$p_q = \frac{N_c}{3} \frac{n_f}{\pi^2} \left[\Phi_{\nu} \left(a_q - \frac{\mu}{T} \right) + \Phi_{\nu} \left(a_q + \frac{\mu}{T} \right) \right] \quad (48)$$

$$p_{gl} = \frac{N_c^2 - 1}{3\pi^2} \int_0^{\infty} \frac{z^3 dz}{e^{z+a_{gl}} - 1} \quad (49)$$

with $a_q = V_1(T)/2T$, $a_{gl} = \frac{9}{4}a_q$ and

$$\Phi_{\nu}(a) = \int_0^{\infty} \frac{z^4}{\sqrt{z^2 + \nu^2}} \frac{dz}{e^{\sqrt{z^2 + \nu^2} + a} + 1} \quad (50)$$

In the paper we consider the case of $\mu = 0$ and characteristic temperature region of $T \approx T_c$ ($T_c = 170 \div 270$ MeV) where quark masses do not affect the thermodynamical functions appreciably. This is due to the fast convergence of the sum over n at large n ensured by factors $\frac{1}{n^4}$, L^n ($L < 1$) while $\varphi_q^{(n)} \approx 1$ for $n \approx 1$. Characteristically, $\varphi_q^{(n)}(m_q = 0) = 1$, and for $m_q = 0.4T$ one has $\varphi_q^{(1)} = 0.96$, $\varphi_q^{(15)} = 0.03$. Therefore one can with a good accuracy neglect masses in (48),(49):

$$p_q = \frac{2n_f}{\pi^2} \int_0^{\infty} \frac{z^3 dz}{e^{z+a_q} + 1} \quad (51)$$

$$p_{gl} = \frac{8}{3\pi^2} \int_0^{\infty} \frac{z^3 dz}{e^{z+a_{gl}} - 1} \quad (52)$$

Eqs. (51),(52) are compared with lattice pressure data in Fig.2 for $n_f = 2 + 1$ (left) and $n_f = 3$ (right figure). In Fig.3 are shown our calculated curves for the cases $n_f = 2 + 1$ (left part) and $n_f = 3$ (right part), which are compared with lattice data from [30].

² The form (48) was independently obtained by N.O. Agasian (to be published).

To simplify further one can use for $\mu = 0$ instead of (51),(52) the first terms of expansion in (44),(45), namely:

$$p_q = \frac{12n_f}{\pi^2} L_{fund} \quad (53)$$

$$p_g = \frac{16}{\pi^2} L_{adj} \quad (54)$$

Another useful quantities to compare with lattice data are the internal energy density and the “nonideality” of the QGP:

$$\varepsilon = T^2 \frac{\partial}{\partial T} \left(\frac{P}{T} \right)_V = \varepsilon_q + \varepsilon_{gl} \quad (55)$$

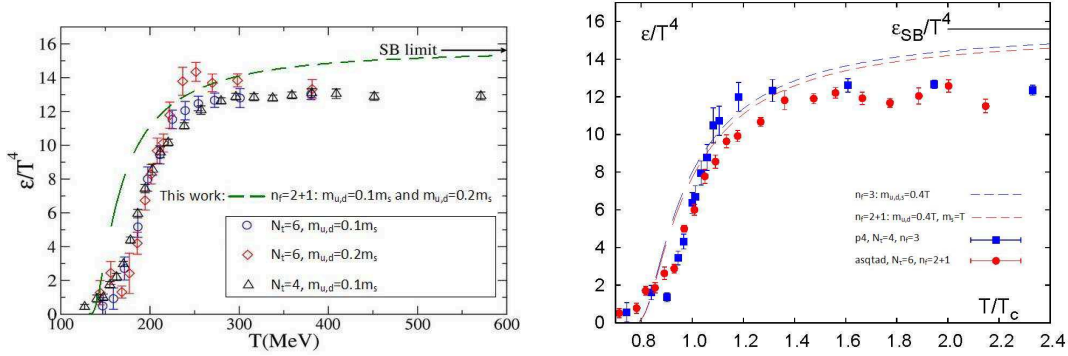


Fig. 4. Energy density $\frac{\varepsilon}{T^4}$ as function of temperature T . The case $n_f = 2 + 1$ with $m_{u,d} = 0.1m_s$ and $m_{u,d} = 0.2m_s$ (green dashed curve) (55) is compared to lattice data from [29](left fig.). The case $n_f = 2 + 1$ with $m_{u,d} = 0.4T$, $m_s = T$ (red dashed curve) and $n_f = 3$ with $m_q = 0.4T$ (blue dashed curve) (55) are compared to lattice data from [28](right fig.).

Using (48),(49) one has

$$\varepsilon_q^{(0)} = \sum_{n_f} \frac{2}{\pi^2} T^2 \frac{d}{dT} \left(T^3 \int_0^\infty \frac{z^4}{\sqrt{z^2 + \nu^2}} \frac{dz}{e^{\sqrt{z^2 + \nu^2} + a_q} + 1} \right) \quad (56)$$

$$\varepsilon_{gl}^{(0)} = \frac{3}{3\pi^2} T^2 \frac{d}{dT} \left(T^3 \int_0^\infty \frac{z^3 dz}{e^{z + a_{gl}} + 1} \right) \quad (57)$$

and the “nonideality” of the QGP:

$$I(T) = \frac{\varepsilon - 3P}{T^4} = T \frac{\partial p}{\partial T} \quad (58)$$

In the simple approximation (53),(54) one has

$$I(T) = \frac{12n_f}{\pi^2} T \frac{dL_{fund}}{dT} + \frac{16}{\pi^2} T \frac{dL_{adj}}{dT} \quad (59)$$

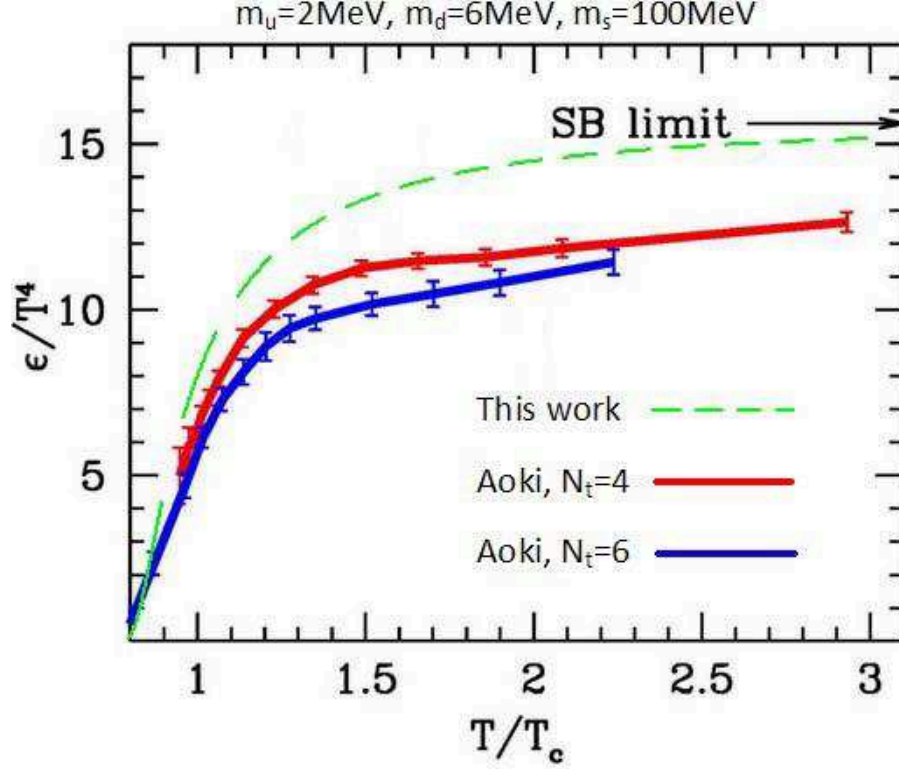


Fig. 5. Energy density $\frac{\epsilon}{T^4}$ as function of temperature T . The curve for $n_f = 3$ with $m_u = 2\text{MeV}, m_d = 6\text{MeV}, m_s = 100\text{MeV}$ (green dashed) (55) is compared to lattice data from [31].

We compare our calculations for $\frac{\epsilon}{T^4}$ in Fig.4 and 5 with three different lattice data: [28],[29],[31]. In Fig.6 we demonstrate our $I(T)$ computed from (58),(51),(52) with lattice data of 2+1 flavor from [31] (left curve) and from [29] (right curve).

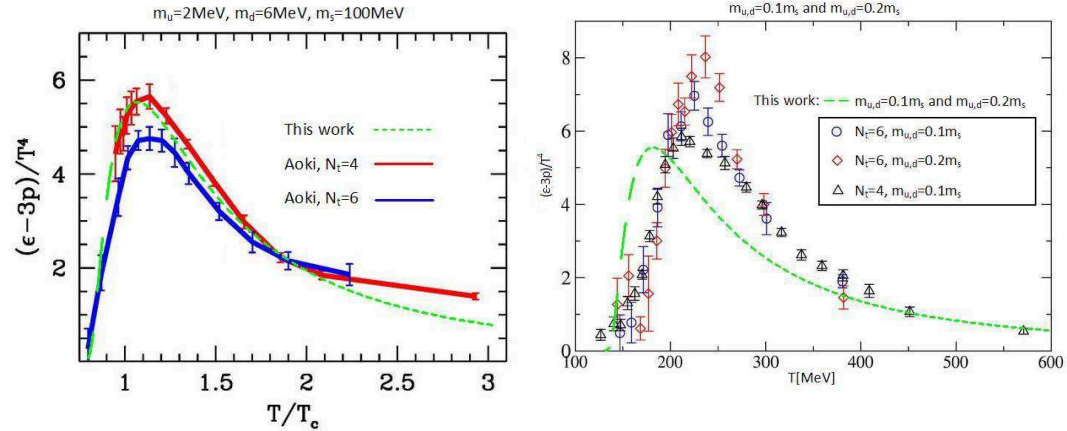


Fig. 6. "Nonideality" of QGP $(\epsilon - 3p)/T^4$. Shown are the curves for (left fig.) $n_f = 3$ with $m_u = 2\text{ MeV}, m_d = 6\text{ MeV}, m_s = 100\text{ MeV}$ (green dashed line) compared to [31] and (right fig.) for $n_f = 2 + 1$ with $m_{u,d} = 0.1m_s$ and $m_{u,d} = 0.2m_s$ compared to [29]. Analytical calculations are done using (48),(49),(55).

At this point it is instructive to estimate the contribution of $q\bar{q}$, gg interactions to the pressure. Writing the virial coefficient in the form $P_j = P_j^{(0)}(1 + \frac{P_j^{(0)}}{T}B_j(T) + \dots)$, where $P_j^{(0)} = P_q, P_{gl}$ in SLA, Eqs. (21),(22), with

$$B_j(T) = \frac{1}{2} \int (1 - e^{U_j(r,T)/T}) dV, j = \text{fund, adj} \quad (60)$$

and taking for $q\bar{q}$ and gg interaction term U_{fund} and U_{adj} respectively at large T as $U_j(r, T) = T u_j(rT)$, one obtains a corrected pressure

$$P = P_q^{(0)}(1 - c_q) + P_{gl}^{(0)}(1 - c_{gl}) \quad (61)$$

where $c_{gl} \cong \frac{16}{\pi^2} \int_0^\infty \rho^2 d\rho (e^{|u_{adj}(\rho)|} - 1)$, $c_q \cong \frac{12n_f}{\pi^2} \int_0^\infty \rho^2 d\rho (e^{|u_{fund}(\rho)|} - 1)$. Note that $q\bar{q}$ and gg interaction in the singlet color state is attractive, so that $|U_j| = -U_j$. The dependence on rT in u_j occurs at large T , in the dimensionally reduced regime, when dynamical dimensional quantity is the spatial string tension $\sigma_H = \text{const} \cdot T^2$, and the Debye mass $m_D(T) \cong 2\sqrt{\sigma_H} = \text{const} \cdot T$.

Thus one expects that 1) the corrected pressure is smaller than the SLA predicts, 2) the large T behavior of $P(T)$ is below the Stefan-Boltzmann values (modulo logarithmic factors). Both features are clearly seen in the Fig.2,3,4,5.

5 Discussion of results. Conclusions.

We have shown in section 2, following [2], that EoS in the zeroth approximation is represented by free quark and gluon lines augmented by the factors L_{fund} for quarks and L_{adj} for gluons. These factors have been derived from the Gaussian color-electric correlators $D^E(x)$, $D_1^E(x)$, and the latter in its turn can be computed analytically from the gluelump Green's function, or directly on the lattice [8,9]. This representation of L_{adj} and L_{fund} allows to express L_j , $j = fund, adj$ in terms of the NP static potential $V_1(r, T)$ at $r = \infty$, and compare the latter with the singlet free energy $F_{Q\bar{Q}}^1(r, T)$. It was argued that V_1 and $F_{Q\bar{Q}}^1$ differ due to presence of excited Qg^n states in $F_{Q\bar{Q}}^1$, and can be taken equal in the first approximation. This leads to the identification of L_j with the modulus of corresponding Polyakov lines. In the Gaussian approximation for V_1 one then automatically obtains the Casimir scaling for L_j : $L_{adj} = (L_{fund})^{\frac{C_2(adj)}{C_2(fund)}}$ which is observed on the lattice with good accuracy [4]. Corrections are found to be of two types: 1) contribution of higher correlators to V_1 and L_j yields less then 10% (20) and can be neglected 2) contribution of excited states yields corrections not connected by Casimir scaling and therefore high accuracy of data [4] imposes a stringent limit on the role of excited states of the type (Qg^n) . For $T > T_c$ our expression (29) automatically predict vanishing of L_{fund} for $n_f = 0$ and behavior of $L_{adj} \cong \exp(-M_0/T)$ with M_0

- lowest gluelump mass ≈ 1 GeV. These features are in good agreement with the lattice data [4], and are shown in Fig.1.

For EoS using formulas of section 2 and treatment in [2] we have given two types of expressions for the pressure P : 1) as a sum over winding n (Matsubara frequencies) in (44), (45) and equivalent forms as integrals over "momentum" z in (48),(49). It was argued that for $\mu = 0$ and not large T , $T_c \leq T \lesssim 2T_c$ one can use much simpler forms of (53),(54), which are first terms of the sums (44),(45).

In all these forms the only source of non-perturbative dynamics in EoS is Polyakov factors L_j , which are defined independently and therefore our EoS is the explicit prediction without any model of fitting parameters. Hence check of our approach is the check of our basic principle that non-perturbative dynamics enters in the form of vacuum based factors L_j .

Comparison of our EoS, (44),(45) or (48),(49), is done with several lattice groups for each quantity, to have an idea of accuracy of our results and of lattice data, and dependence on quark masses. The latter appears very weak in EoS, e.g. quark mass of $m_q = 0.4T$ yields a 4% correction to the zero mass result, while on the lattice this dependence is stronger. We compare pressure $\frac{P}{T^4}$ for $n_f = 0, 2, 3$ and $m_q = 0.4T$ in Fig.3 (left part). One can see deviation of $\sim 20\%$ of our curves from lattice data [28] for $T \lesssim 3T_c$ and the same type of agreement for $n_f = 2 + 1$ with data from [29]. Typically our curves are higher with the fact that the (attractive) interaction between quarks, antiquarks and gluons is not taken into account. The first correction (60),(61) treating this attraction between $q\bar{q}$ and gg , has the negative sign, which might improve the agreement. The agreement is however better with another set of lattice data from [30] done for $n_f = 2 + 1$, see Fig.3. Comparing left and right parts of the Fig.3 one can notice, that lattice data [30] are much more sensitive to the quark masses, than our prediction.

Another interesting comparison is for the internal energy ε and non-ideality $I = \frac{\varepsilon - 3P}{T^4}$, given in Fig.4,5 and 6. It is important that both quantities contain derivatives $T \frac{dL_j(T)}{dT}$ and therefore are much more sensitive to the type of non-perturbative dynamics, which is present in our approach. The agreement of our Eqs. (56),(57) with data from [28] and [29] are shown in Fig.4 and is of the same quality as for the pressure: one has $\sim 15\%$ higher theoretical curve for $T > 1.2T_c$, the same one can see in Fig.5 with data from [31]. Note, that the quark masses in this case are close to physical ones. Finally, the non-ideality is compared to the data from [31] in the left part of Fig.6 and is in good agreement with data [29] (right part of Fig.6 is less successful, because lattice data from [29] and [31] differ strongly). As a whole, it is surprising that such simple approach without any parameters (actually primitive formulas (53),(54) already have sufficient accuracy within our approximation) yields a

reasonable agreement with lattice data for $P(T)$, $\varepsilon(T)$ and $I(T)$. If one adds to that a good agreement of our phase curve $T_c(\mu)$ in [5] with majority of lattice data, the possible conclusion might be, that our zeroth approximation to the non-perturbative vacuum fields - taking non-perturbative contribution in the form of L_j - is a viable approach to the dynamics of QGP. The next step is an account of possible perturbative and non-perturbative interactions between quarks, antiquarks and gluons, which is partly done in [3,9] for color-electric fields ($V_1(r, T)$) and in [20] for color-magnetic ones. The exact contribution of these effects to the EoS is not yet done and should be an important next step. The strong interaction in $(q\bar{q})$ and (gg) systems discovered in [20] might give further support for the idea of strong quark-gluon plasma - sQGP.

The authors are indebted for useful discussions to members of ITEP and FIAN physical seminars. We are also grateful to S.N.Fedorov for providing us with a useful program "GetData". The financial support of the RFFI grant 06-02-17012 and NSh-843.2006.2 is acknowledged. This work was supported by the Federal Agency for Atomic Energy of Russian Federation.

References

- [1] J.-P.Blaizot, Plenary talk at QM 2006, Shanghai, hep-ph/0703150;
B.Müller, J.L.Nagle, *Ann. Rev. Nucl. Part. Phys.* **1**, (2006); nucl-th/0602029.
- [2] Yu.A.Simonov, *Ann. Phys.* (to be published), hep-ph/0702266.
- [3] Yu.A.Simonov, *Phys. Lett.* **B619** (2005), 293.
- [4] S.Gupta, K.Hübner, O.Kaczmarek, hep-lat/0608014.
- [5] Yu.A.Simonov, M.A.Trusov, *Phys. Lett.* **B** (in press), hep-ph/0703277;
hep-ph/0703228.
- [6] M.Shifman, A.Vainshtein, V.Zakharov, *Nucl. Phys.* **B147**, 385, 448 (1979);
O.Andreev, V.I.Zakharov, hep-ph/0703010.
- [7] Yu.S.Simonov, *Phys.Atom. Nucl.* **69**, (2006), 528; hep-ph/0501182.
- [8] A.Di Giacomo, E.Meggiolaro, H.Panagopoulos, *Nucl. Phys.* **B483** (1997), 371;
M.D'Elia, A.Di Giacomo, E.Meggiolaro, *Phys. Rev.* **D67**, (2003), 114504.
- [9] A.Di Giacomo, E.Meggiolaro, Yu.A.Simonov, A.I.Veselov, hep-ph/0512125,
Phys. Atom. Nucl. (in press).
- [10] Yu.A.Simonov, *JETP Lett.* **54**, 249 (1991); **55**, 627 (1992);
N.O.Agasian, *JETP Lett.* **57** (1993), 200; *Phys. Lett.* **B562** (2003), 257.
- [11] H.G.Dosch, *Phys. Lett.* **B190**, (1987), 177; H.G.Dosch, Yu.A.Simonov, *Phys. Lett.* **B 205**, (1988), 339; Yu.A.Simonov, *Nucl. Phys.* **B 307**, (1988), 512; A.Di

- Giacomo, H.G.Dosch, V.I.Shevchenko, Yu.A.Simonov, *Phys. Rep.* **372**, (2002), 319.
- [12] Yu.A.Simonov, *Nucl. Phys.* **B592** (2001), 350.
- [13] M.Foster, C.Michael, *Phys. Rev.* **D59**, (1999), 094509.
- [14] B.S.De Witt, *Phys. Rev.* **162** (1967), 1195, 1239;
J.Honerkamp, *Nucl. Phys.B* **48**(1972), 269;
G.'t Hooft *Nucl. Phys.B* **62** (1973), 444, “Lectures at Karpacz”, in: *Acta Univ. Wratislaviensis* **368** (1976), 345;
L.F.Abbot, *Nucl. Phys. B* **185** (1981), 189.
- [15] Yu.A.Simonov, *Phys. At Nucl.* **58** (1995), 107, hep-ph/9311247;
JETP Lett. **75** (1993), 525; Yu.A.Simonov, in: “Lecture Notes in Physics”(H.Latal and W.Schwinger, Eds.) Vol.479, p. 139, Springer, 1996.
- [16] Yu.A. Simonov, *Phys. At. Nucl.* **58**, (1995), 309, hep-ph/9311216
- [17] E.V. Komarov, Yu. A. Simonov (in preparation).
- [18] Yu.A. Simonov, J.A. Tjon , *Ann. Phys.* **228**, 1 (1993), ibid 300, 54 (2002)
- [19] N.G.Van Kampen, *Phys. Rep. C* **24** (1976), 171.
- [20] A.V. Nefediev, Yu.A. Simonov, *Phys. At. Nucl.*(in press), hep-ph/0703306
- [21] P.Petretzky, Plenary talk at Lattice 2004, hep-lat/0409139
- [22] V.I. Shevchenko, Yu.A. Simonov, *Phys. At. Nucl.* **60**, (1997), 1201.
- [23] V.I.Shevchenko, Yu.A.Simonov, *Phys. Rev. Lett.* **85** (2000), 1811, *Int.J. Mod. Phys. A* **18** (2003, 127);
G.S.Bali, *Phys. Rev. D* **62** (2000), 114503;
S.Deldar, *Phys. Rev. D* **62** (2000), 034509.
- [24] O.Kaczmarek, F.Zantov, *Phys. Rev. D* **71** (2005), 114510; M.Döring, S.Ejiri, O.Kaczmarek, F.Karsch, E.Laermann, hep-lat/0509150.
- [25] N.O. Agasian, Yu.A. Simonov, *Phys. Lett. B* **639**, (2006), 82.
- [26] O.Kaczmarek, F.Karsch, P.Petreczky, F.Zantov, *Phys. Lett. B* **543** (2002), 41; hep-lat/02007002; F.Zantov, O.Kaczmarek, F.Karsch, P.Petreczky, hep-lat/0110103.
- [27] O. Kaczmarek, F. Zantow, hep-lat/0506019
- [28] F.Karsch, *J.Phys.Conf.Ser.* **46** (2006) 122-131, arXiv:hep-lat/0608003
- [29] C.Bernard et al., arXiv:hep-lat/0610017v1
- [30] F.Karsch, arXiv:hep-ph/0701210v1
- [31] Y.Aoki, Z.Fodor, S.D.Katz, K.K. Szabo, *JHEP* **0601** (2006) 089, arXiv:hep-lat/0510084v2